LAWRENCE
LIVERMORE
NATIONAL
LABORATORY

LLNL-PROC-520234

Dislocation Dynamics Simulations of Junctions in Hexagonal Close-Packed Crystals

C. Wu, S. Aubry, P. Chung, A. Arsenlis

December 13, 2011

MRS Fall 2011
Boston, MA, United States
November 28, 2011 through December 2, 2011

Report Documentation Page

Form Approved
OMB No. 0704-0188

1. REPORT DATE	2. REPORT TYPE	3. DATES COVERED
13 DEC 2011		**00-00-2011 to 00-00-2011**

4. TITLE AND SUBTITLE	5a. CONTRACT NUMBER
Dislocation Dynamics Simulations of Junctions in Hexagonal Close-Packed Crystals	5b. GRANT NUMBER
	5c. PROGRAM ELEMENT NUMBER
6. AUTHOR(S)	5d. PROJECT NUMBER
	5e. TASK NUMBER
	5f. WORK UNIT NUMBER
7. PERFORMING ORGANIZATION NAME(S) AND ADDRESS(ES) **US Army Research Laboratory,Computational and Information Sciences Directorate,Aberdeen Proving Ground,MD,21005**	8. PERFORMING ORGANIZATION REPORT NUMBER
9. SPONSORING/MONITORING AGENCY NAME(S) AND ADDRESS(ES)	10. SPONSOR/MONITOR'S ACRONYM(S)
	11. SPONSOR/MONITOR'S REPORT NUMBER(S)

12. DISTRIBUTION/AVAILABILITY STATEMENT
Approved for public release; distribution unlimited

13. SUPPLEMENTARY NOTES
Presented at the Materials Research Society (MRS) Fall Meeting, November 28, 2011 through December 2, 2011, Boston, MA

14. ABSTRACT
The formation and strength of dislocations in the hexagonal closed packed material beryllium are studied through dislocation junctions and the critical stress required to break them. Dislocation dynamics calculations (using the code ParaDiS) of junction maps are compared to an analytical line tension approximation in order to validate our model. Results show that the two models agree very well. Also the critical shear stress necessary to break 30o - 30o and 30o - 90o dislocation junctions is computed numerically. Yield surfaces are mapped out for these junctions to describe their stability regions as function of resolved shear stresses on the glide planes. The example of two non-coplanar binary dislocation junctions with slip planes [2-1-10] (01-10) and [-12-10] (0001) corresponding to a prismatic and basal slip respectively is chosen to verify and validate our implementation.

15. SUBJECT TERMS

16. SECURITY CLASSIFICATION OF:			17. LIMITATION OF ABSTRACT	18. NUMBER OF PAGES	19a. NAME OF RESPONSIBLE PERSON
a. REPORT **unclassified**	b. ABSTRACT **unclassified**	c. THIS PAGE **unclassified**	**Same as Report (SAR)**	**8**	

Disclaimer

Dislocation Dynamics Simulations of Junctions in Hexagonal Close-Packed Crystals

Chi-Chin Wu [1,2*], Sylvie Aubry [3], Peter Chung[2], Athanasios Arsenlis[3]
[1]Oak Ridge Affiliated Universities Maryland, 4692 Millennium Drive, Suite 101, Belcamp MD 21017, U.S. A.
[2]Computational and Information Sciences Directorate, US Army Research Laboratory, Aberdeen Proving Ground, MD 21005, U.S.A.
[3]High Performance Computational Materials Science and Chemistry Group Condensed Mater and Materials Division Lawrence Livermore National Laboratory P.O. Box 808, L-367 Livermore, CA 94551, U.S.A.
[*]Email: chi-chin.wu.ctr@mail.mil

ABSTRACT

The formation and strength of dislocations in the hexagonal closed packed material beryllium are studied through dislocation junctions and the critical stress required to break them.

Dislocation dynamics calculations (using the code ParaDiS) of junction maps are compared to an analytical line tension approximation in order to validate our model. Results show that the two models agree very well. Also the critical shear stress necessary to break 30^o - 30^o and 30^o - 90^o dislocation junctions is computed numerically. Yield surfaces are mapped out for these junctions to describe their stability regions as function of resolved shear stresses on the glide planes.

The example of two non-coplanar binary dislocation junctions with slip planes [2-1-10] (01-10) and [-12-10] (0001) corresponding to a prismatic and basal slip respectively is chosen to verify and validate our implementation.

INTRODUCTION

Dislocation mechanisms in hexagonal closed packed (HCP) crystals are more complex than those in cubic systems such as face-centered cubic (FCC) and body-centered cubic (BCC) crystals due to the reduced crystal symmetry and different slip modes caused by the hexagonal lattice and material-dependent *c*/*a* ratios (where *c* and *a* are the lattice spacing on the basal plane and its normal direction, respectively). Instead of unanimously gliding on the close-packed basal planes (0001) as all dislocations do in FCC and BCC, the slip systems for dislocations in HCP also involve higher-order non-basal slip planes including {1 0 -1 0} prismatic, first-order {10-11} pyramidal, and second-order {11-22} pyramidal slip planes, and several possible Burgers vectors including <11-20>, <0001>, or <11-2-3> [1-2]. Despite of these complexities, the HCP structure and all slip systems and cross-slip planes can still be conveniently described by employing a simple three-index orthogonal coordinate system based on the double tetrahedron notation for DD simulations [3-4]. In plastic deformation, dislocation junctions can form energetically (the so called "zipping" phenomena) but also can be destroyed via "unzipping" by an applied stress [5-15]. When an external stress is applied, all dislocation segments involved in the junction may bow out via Frank-Read (F-R) mechanism. The changing strain/stress field surrounding dislocations induced by the dynamically changing dislocation configurations would affect the process of junction unzipping. In a large dislocation network, a junction often becomes an obstacle for dislocation motions and interactions. Therefore, junction-related phenomena directly affect local dislocation microstructures and the collective properties of the entire

dislocation network such as dislocation density. By using a modified DD code, Parallel Dislocation Dynamics Simulator (ParaDiS) assuming isotropic mobility and linear isotropic elasticity, this work investigates conditions for manipulating the formation and destruction of binary junctions in HCP crystals using the [2-1-10] (01-10) and [-12-10] (0001) slip systems [16]. Junction formation from two intersecting dislocations is mapped along with two other possible final configurations, crossed-state and repulsion, as function of initial dislocation orientations. For junctions formed by the 30^o - 30^o and 30^o - 90^o intersecting dislocations, various stress fields from different loading directions and magnitudes are repeatedly loaded to test their strengths and the results are shown as yield surfaces as function of resolved shear stresses on the glide planes. We select to use Be as an example of HCP metals.

SIMULATION METHOD

Instead of using the four Miller-Bravais indices for HCP, the coordinates of atomic positions in HCP are indexed with three orthogonal axes, using a double-tetrahedral notation similar to the Thompson Tetrahedral for FCC [2, 4]. Two long straight dislocations $\boldsymbol{\xi_1}$ and $\boldsymbol{\xi_2}$ gliding with different slip systems intersect each other at the midpoint. In our models, dislocations of equal lengths equivalent to 40,000 times of the lattice spacing with pinned end nodes are given with initial orientations to the intersection edge of glide planes varying from -180^o to $+180^o$ of 30^o increment. In ParaDiS, the end nodes are extended using virtual segments to simulate two intersecting dislocations of infinite lengths. The slip systems used for dislocations $\boldsymbol{\xi_1}$ and $\boldsymbol{\xi_2}$ having Burger vectors $\mathbf{b_1}$ and $\mathbf{b_2}$, respectively, are listed in Table 1. The dislocations are then allowed to interact for 30,000 total timesteps. When a junction is formed energetically, the direction of junction $\mathbf{e_x}$ is normal to both glide planes so that $\mathbf{e_x} = \mathbf{n_1} \times \mathbf{n_2}$ where $\mathbf{n_1}$ and $\mathbf{n_2}$ are the normal directions to glide planes 1 and 2, respectively, as shown in Fig. 1. The Burgers vector $\mathbf{b_3}$ for the junction is therefore $\mathbf{b_1} + \mathbf{b_2} = [1\ 0\ 0]$ in our 3-index coordinate system, making the junction sessile because it is not a slip direction on either slip plane. The normal to the junction, $\mathbf{n_3}$, is $\mathbf{b_3} \times \mathbf{e_x} / |\mathbf{b_3}|$.

Table 1. The slip systems used for intersecting dislocations in HCP.

Dislocation	Slip system	4-index notation: The Miller-Bravais system	3-index notation The orthogonal axes used in this work
$\boldsymbol{\xi_1}$	Prismatic slip plane $\mathbf{n_1}$	(0 1 -1 0)	($\sqrt{3}$/2 1/2 0)
	Burgers vector $\mathbf{b_1}$	1/3[2 -1 -1 0]	[1/2 -$\sqrt{3}$/2 0]
$\boldsymbol{\xi_2}$	Basal slip plane $\mathbf{n_2}$	(0 0 0 1)	(0 0 1)
	Burgers vector $\mathbf{b_2}$	1/3[-1 2 -1 0]	[1/2 $\sqrt{3}$/2 0]

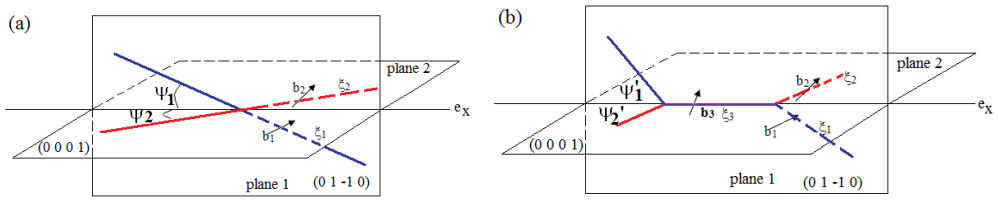

Fig.1. A sketch showing two intersecting straight dislocations $\boldsymbol{\xi_1}$ and $\boldsymbol{\xi_2}$: (a) before and (b) after the formation of junction. In (a), $\boldsymbol{\xi_1}$ and $\boldsymbol{\xi_2}$ are oriented to $\mathbf{e_x}$ with $\boldsymbol{\psi_1}$ and $\boldsymbol{\psi_2}$ angles on planes $\mathbf{n_1}$ and $\mathbf{n_2}$, respectively. In (b), the junction $\boldsymbol{\xi_3}$ carries a Burgers vector $\mathbf{b_3}$, a sum from $\mathbf{b_1}$ and $\mathbf{b_2}$, and the angles change to $\boldsymbol{\psi_1}$' and $\boldsymbol{\psi_2}$' for $\boldsymbol{\xi_1}$ and $\boldsymbol{\xi_2}$, respectively.

The applied stress $\boldsymbol{\sigma}$ for breaking the junction is calculated as $\sigma = \alpha\, s_1 + \beta\, s_2 + \gamma\, s_3$ where $\mathbf{s_1}$, $\mathbf{s_2}$, and $\mathbf{s_3}$, are the projection 3x3 matrices on dislocation $\boldsymbol{\xi_1}$, dislocation $\boldsymbol{\xi_2}$, and the dislocation junction $\boldsymbol{\xi_3}$, respectively and α, β, and γ are their respective resolved shear stresses. They are scalar magnitudes in the unit of GPa. In this form, $\mathbf{s_1}$, $\mathbf{s_2}$, and $\mathbf{s_3}$ are not independent from one another. We can define $\mathbf{S_1}$, $\mathbf{S_2}$, and $\mathbf{S_3}$ such that [18]

$$S_i s_i = I$$
$$S_i s_j = 0,\ i \neq j$$

where i and j vary in {1, 3}. The coefficient γ is set to zero preventing the junction from bowing out. This forces the junction to only be destroyed via unzipping along a straight junction line. Different ratios between $\mathbf{S_1}$ and $\mathbf{S_2}$ are used and applied repeatedly with incrementally increasing magnitudes to junctions formed by 30^o-30^o and 30^o-90^o dislocations until the junctions can be completely destroyed and the locked dislocations $\boldsymbol{\xi_1}$ and $\boldsymbol{\xi_2}$ can glide on their respective slip planes again. The extent of junction unzipping is recorded with the increasing applied stress as unzipping ratio, calculated by λ/λ_o where λ and λ_o are the destroyed junction length and the initial junction length, respectively. Many critical pairs of α and β values just unzipping the junctions obtained by extensive numbers of simulations are then used to construct the yield surfaces of junction as function of $\mathbf{S_1}$ and $\mathbf{S_2}$. The elastic constants for Be are a shear modulus equals to 130 GPa, a Poisson's ratio of 0.032, c/a=1.568 with a lattice constant a=2.29nm. The core radius of dislocation is taken as half of the lattice spacing. The dislocations are modeled in the center of a cubic space of 60 micrometer cube.

RESULTS AND DISCUSSIONS

Mapping of junction formation by dislocation intersection

Depending on the initial angle the intersection dislocations make with the junction direction, three mechanisms can happen. A junction can form via zipping from the intersecting point along the intersection line, the dislocations may form a cross-state, or the dislocations may repel each other. Fig. 2 is a mapping of these resultant dislocation configurations as function of $\boldsymbol{\psi_1}$ and $\boldsymbol{\psi_2}$, the angles the dislocations make with the junction direction $\mathbf{e_x}$ respectively. Symbols represent DD results whereas shaded regions correspond to line tension approximations. In the DD simulations, 13 x 13 different angles are chosen for $\boldsymbol{\psi_1}$ and $\boldsymbol{\psi_2}$ and 100 x 100 angles are chosen for the analytical results. As shown in the figure, the DD-simulated results agree very well with analytical results from the line tension approximation [12-13]. The regions of junction formation show excellent mirror symmetries about the axes and diagonals, similar to those reported for BCC and FCC [11, 13-14]. This can be attributed to the particular choice of the equal magnitudes (one lattice spacing) for the Burgers vectors $\mathbf{b_1}$ and $\mathbf{b_2}$ used for dislocations $\boldsymbol{\xi_1}$ and $\boldsymbol{\xi_2}$, respectively, and the resultant Burgers vector $\mathbf{b_3}$ for the junction $\boldsymbol{\xi_3}$. In addition, the near zero value for beryllium's Poisson ratio also adds symmetry to the calculation results.

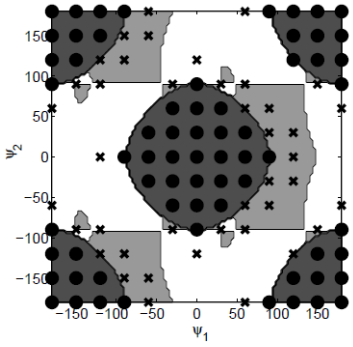

Fig.2. Map of the final configurations of two intersecting dislocations: analytical results are represented in dark, gray and white regions corresponding to junction formation, crossed-states and repulsive states, respectively. Dots and crosses are DD-simulated results from this work representing junction formation and crossed-states, respectively. ψ_1 and ψ_2 are the initial angles to the intersection edge of glide planes for dislocations ξ_1 and ξ_2, respectively.

Mapping of junction destruction by applied stress

Fig. 3 shows the yield surfaces for the junctions formed by 30^o - 30^o and 30^o - 90^o dislocations as function of $\mathbf{S_1}$ and $\mathbf{S_2}$, the stresses applied to dislocations ξ_1 and ξ_2 on slip planes 1 and 2, respectively. We observe a symmetry about the $\mathbf{S_1} = -\mathbf{S_2}$ line for the 30^o - 30^o junction to about the $\mathbf{S_1} = \mathbf{S_2}$ line for the 30^o-90^o junction. Such symmetries are expected considering the equal Burgers vector magnitudes and the low Poisson ratio used in this work. The symmetry about the diagonal of applied stresses for a yield surface of junction has also been observed for high symmetry crystals such as FCC and BCC even though the shapes are often more slanted [9, 10-12]. As shown in Fig. 3, both junctions would be stable under an applied stress of ~ 50 MPa.

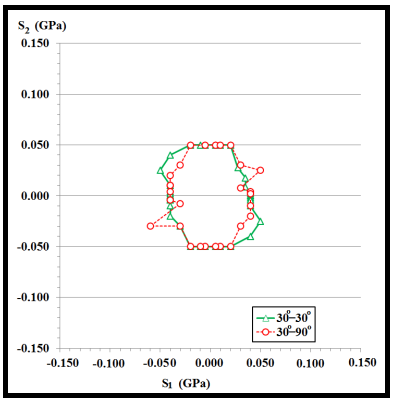

Fig.3. Yield surfaces of 30^o-30^o and 30^o-90^o junctions on the prismatic/basal planes. $\mathbf{S'_1}$ and $\mathbf{S'_2}$ are the stresses applied to dislocations ξ_1 and ξ_2 on slip planes 1 and 2,

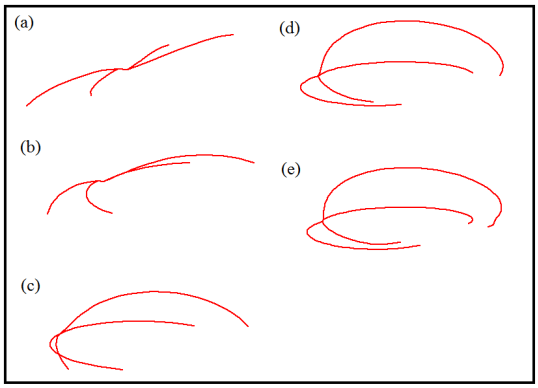

Fig.4. Image sequences showing the unzipping of 30^o-90^o junction by the applied stresses $\mathbf{S_1} = \mathbf{S_2} = 30$ MPa.

Unzipping mechanisms of junctions

Several interesting phenomena are noticed during junction unzipping from our DD simulations. The unzipping evolves with varying speed. As shown from images (a) to (e) in Fig. 6 for the unzipping of 30^o-30^o junction using an applied stresses of $\alpha = \beta = -30$MPa, the junction appears to translate during unzipping until it is completely destroyed due to the faster movement of node “a” than node “b”. The breaking of 30^o-30^o junction also proceeds smoothly but at a relatively slow speed followed by a dramatically increased speed after both junction joints are within a certain range. However, the unzipping would slow down again when the junction nodes

are so close that the network assembles a "crossed-state" with only a tiny segment of junction remains prior to complete destruction of junction. This heterogeneous velocity across the unzipping process can be attributed to the combined effects by the varying junction length and segment-segment forces. Moreover, local dislocation turning and rotation is evident in DD simulations during junction unzipping due to the F-R mechanism of dislocations, as shown from images (a) to (c) in Fig. 4.

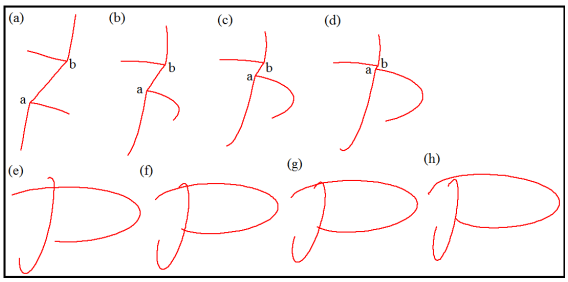

Fig.6. Image sequences showing the unzipping of 30^o-30^o junction by the applied stresses $\mathbf{S_1} = \mathbf{S_2} = -0.030$GPa.

CONCLUSIONS

The formation and destruction of non-coplanar binary junctions in HCP have been investigated using [2-1-10] (01-10) and [-12-10] (0001) slip systems. The junction formation regions across all possible initial dislocation orientations and the yield surfaces of 30^o-30^o and 30^o-90^o junctions show good symmetries due to the equal Burgers vectors and the low Poisson ratio used. Several interesting junction unzipping mechanisms including junction translation and local turning and rotation of dislocations are identified from DD simulations.

ACKNOWLEGEMENT

This work is performed with supports from the Oak Ridge Affiliated Universities in Maryland, the U.S. Army Research Laboratory Enterprise for Multi-scale Research of Materials, the DoD High Performance Supercomputing Resource Center, and the LC system at the DoE Lawrence Livermore National Laboratory. This work performed under the auspices of the U.S. Department of Energy by Lawrence Livermore National Laboratory under Contract DE-AC52-07NA27344.

REFERENCES

1. J. P. Hirth and J. Lothe, *Theory of Dislocations*, 2nd ed. Krieger Publishing Company (1982).
2. D. Hull and D. J. Bacon, *Introduction to Dislocations*, Elsevier (2001).
3. V.V. Damiano, *Transactions of the Metallurgical Society of AIME*, **227**, 788 (1963).
4. Y. A. Osipyan and I. S. Smirnova, *J. Phys. Chem.. Solids*, **32**, 1521 (1971).
5. J. P. Hirth, *J. Appl. Phys.* **32**, 700 (1961).
6. B. Devincre, L. P. Kubin, *Modelling Simul. Mater. Sci. Eng.*, **2**, 559 (1994).
7. S. J. Zhou, D. L. Preston, P. S. Lomdahl, D. M. Beazley, *Science*, **279**, 1525 (1998).
8. D. Rodney and R. Phillips, *Phys. Rev. Lett.*, **82**, 1704 (1999).
9. L. K. Wickham, K. W. Schwarz, J. S. Stölken, *Phys. Rev. Lett.*, **83**,4574 (1999).

10. V. B. Shenoy, R. V. Kukta, and R. Phillips, *Phys. Rev. Lett.*, **84**, 1491 (2000).
11. H. M. Zbib, R. D. de la Rubia, M. Rhee, J. P. Hirth, *J. Nucl. Mater.,* **276**, 154 (2000).
12. L. Dupuy L and M. C. Fivel, *Acta Mat.,* 50, 4873 (2002).
13. R. Madec, B. Devincre, L. P. Kubin, T. Hoc, and D. Rodney, *Science*, **301**, 1879 (2003).
14. G. Monnet, B. Devincre, and L. P. Kubin, *Acta Mat.*, **52**, 4317 (2004).
15. L. Capolungo, *Acta Mat.*, **59**, 2909 (2011).
16. A. Arsenlis, W. Cai, M. Tang, M. Rhee, T. Oppelstrup, G. Hommes, T. G. Pierce, and V. V. Bulatov, *Modelling Simul. Mater. Sci. Eng.*, **15**, 553 (2007).
17. R. E. Newnham, *Properties of Materials: Anisotropy, Symmetry, Structure*, Chap. 13, Oxford University Press (2005).
18. E. Martinez, J. Marian, A. Arsenlis, M. Victoria and J. M. Perlado, *J. Mech. Phys. Sol.* 56 p. 869-895 (2008).